Focusing of Smith-Purcell radiation from a two-dimensional particle array in the prewave zone

D. I. Garaev,[1] D. Yu. Sergeeva [1,2] and A. A. Tishchenko [1,2,*]

[1]*International Research Laboratory "Radiation of Charged Particles", National Research Nuclear University*
"MEPhI," Moscow, 115409, Russia
[2]*Laboratory of Radiation Physics, Belgorod National Research University, Belgorod, 308015, Russia*

A generalized theory of Smith-Purcell radiation (SPR) from a two-dimensional (2D) array of subwavelength particles is presented. Unlike most theories of SPR, this one is valid in the prewave zone and the near zone. We have obtained a generalized dispersion relation that determines the points of concentration of radiation in the prewave zone rather than in the ordinary directions of propagation of the most intense radiation; in the wave zone, the dispersion relation transforms into the ordinary one. Analytically, we derived that it is the parabolic law that describes how the individual elements should be arranged for the most intense radiation to be achieved. Interestingly, for the ultrarelativistic limit, the parabolic law turns into the hyperbolic one. Therefore, to focus the radiation from ultrarelativistic electrons in the prewave zone, a hyperbolically arranged 2D grating should be used instead of a rectangular one. Our findings suggest that the radiation intensity at a point of focus in the prewave zone can be sensitive to numerically very small changes in the locations of the individual constituent elements of the array determining the topology—the way the array's elements are arranged. The theory is constructed for particles with arbitrary dielectric properties, including metal ones; numerical analysis has been performed for dielectric particles.

I. INTRODUCTION

Smith-Purcell radiation (SPR) is emitted when electrons move above a periodic structure [1–3]. The fact that the electrons do not scatter on the target makes SPR very attractive not only for nondestructive diagnostics [4–7] of relativistic and ultrarelativistic electron beams, but also for developing on-chip radiation sources based on non- and moderately relativistic electrons [8–13] (see also a fresh comprehensive review [14]).

One of the most modern trends in current research of free-electron radiation is the problem of its shaping. The schemes for radiation beam shaping were proposed for radiation in the microwave [9], terahertz [15], optical [10,11], and recently in the x-ray regime [16]. These proposed schemes are using SPR from custom aperiodic gratings [12]. The most common proposal, which was also recently demonstrated experimentally in the optical regime [11], relied on a grating with a chirp: a metagrating can serve for the emission of converging wavefronts, with different wavelengths converging at different positions. In [17,18] the directions in which Cherenkov radiation could be concentrated are investigated, using conelike targets, while in [13] a focused broadband transition radiation was explored for the structure designed to effectively mimic a porous hemispherical geometry using an engineered planar lens.

All the above-mentioned studies, however, are based on consideration of radiation in the wave zone remote from the radiating structure. It is correct, for example, for diagnostics of moderately relativistic beams, or when we need to know only the radiation characteristics far from the grating. Still, in many applications the characteristics of radiation are required in more near zones: e.g., when the radiation from an on-chip source is used to transfer the signal to the nearby vicinity, or when we need to concentrate the radiation in a certain point at an arbitrary distance from the radiation source. The only exception we know of is reported in Ref. [19], in which the qualitative way was proposed to estimate the concentration of radiation at a certain point that could be not in the wave zone only; yet this qualitative consideration does not describe analytically or experimentally the emitted field in these conditions, intensity, and other radiation characteristics.

Below, we study the characteristics of SPR in the prewave and near zones from relativistic electrons, and analyze the opportunity to control the focusing of SPR, tailoring the structure of a radiating periodic, or near-periodic, two-dimensional (2D) array constructed of separated subwavelength particles. The array can be realized on the submicrometer scale, which supports the optical range, and on the submillimeter scale, which corresponds to terahertz radiation.

II. SMITH-PURCELL RADIATION IN THE PREWAVE ZONE

For a long time SPR was studied only for one-dimensional (1D) systems—i.e., diffraction gratings periodic only along one direction. Comprehensive information about associated experiments and theoretical models can be found in the monographs [2,3]; the major properties of SPR can be seen from the dispersion relation,

$$d_x(\beta^{-1} - \cos\theta) = s_x\lambda, \quad s_x = 1, 2, \ldots, \quad (1)$$

*tishchenko@mephi.ru

which links the only grating period d_x and the relative velocity of the charge β with the wavelength of radiation λ and the polar angle θ. The natural number s_x is called the diffraction order. As the maximum of radiation lies in the plane perpendicular to the grating surface and parallel to the particle's trajectory, the dispersion relation in Eq. (1) can be supplemented by the equality of the azimuthal angle of propagation ϕ to zero:

$$\phi = 0. \tag{2}$$

From the dispersion relation it follows that contrary to usual diffraction radiation, SPR has a strictly ordered spectral-angular distribution of energy: along each direction there is a set of quasimonochromatic lines corresponding to different diffraction orders. One can easily tune the spectral and spatial properties of SPR, adjusting two parameters in Eq. (1): d_x and β. Therefore, by means of the Smith-Purcell mechanism it is possible to get radiation in a wide spectral range, including THz [20], which is not so easy to achieve using traditional sources.

Most of the theoretical approaches describing SPR, including those mentioned above, however, are valid only in the wave (far) zone: the distant area where radiation has the properties of that from a point source. In a relativistic case, for transition radiation it was found that the boundary of the wave zone moves away from the source of radiation linearly with the wavelength λ and quadratically with the Lorentz factor of the charge γ [21]. The same applies to diffraction radiation. Therefore, for long wavelengths and ultrarelativistic electrons (or other charged particles), the wave zone of SPR might be quite large.

The specific criterion for the distance r from a source of SPR, corresponding to the wave zone, was established by Karlovets and Potylitsyn [22]:

$$r \gg \Re. \tag{3}$$

As expected, the quantity $\Re$ is determined by the direction, the wavelength of radiation, and the Lorentz factor. In addition, $\Re$ depends on both the longitudinal L and transverse M dimensions of the 2D array, which we call below a 2D grating as well:

$$\Re = \max\left(\frac{L^2 \sin^2\theta}{\lambda}, \ \frac{\varepsilon^2 \cos^2\phi}{\lambda} \right), \tag{4}$$

where

$$\varepsilon = \min(M, \ \gamma\lambda) \tag{5}$$

corresponds to the effective transverse size of the radiating region. Therefore, Eq. (5) generalizes both cases: when the Coulomb field of radius $\gamma\lambda$ covers the grating completely, and only partially.

At distances $r < \Re$ a complex structure of radiation manifests itself due to the finiteness of the grating, and Eqs. (1) and (2) are no longer applicable. The vicinity of a source ($r < \lambda$), where the nonradiative nature of the field prevails, is usually called the near zone. To designate the region between the wave zone and near zone ($\lambda \ll r < \Re$) we use the term "prewave zone" proposed by Verzilov in regard to transition radiation [21]. Criterion equation (3) actually has a well-known analog
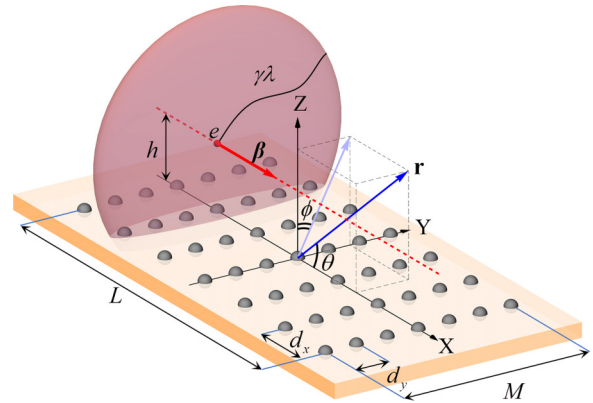
in optics, separating the Fresnel and Fraunhofer diffraction zones [23].

For a better representation of the quantity $\Re$, below we give some examples. According to Eq. (4) for a 5 cm long grating and 1 mm wavelength of radiation, the parameter $\Re$ is equal to or more than 2.5 m in the direction normal to the surface of the grating. This means that for the radiation to be registered in the wave zone, a detector should be located at least at a distance of $r \gg 2.5$ m from the grating. Moreover, in the case of ultrarelativistic electrons, $\Re$ reaches tens of meters for the THz range of radiation. These estimates show that it might be complicated to locate a detector in the wave zone due to simple space limitations for an experimental setup, or an additional optical system might be needed. Therefore, the construction of the prewave zone theory is of great importance.

In fact, Ref. [22] presents such a theory, based on the simple Huygens-Kirchhoff principle, which limits to some extent its applicability, still leaving its results interesting and important. For an ordinary 1D grating of an ideal conductor it predicts spatial and spectral broadening of radiation peaks.

Presently the study of SPR in its wave zone has extended to targets of different topologies. For instance, Ref. [24] contains the theory of SPR from a bigrating surface, and Ref. [25] is devoted to diffraction radiation from aligned nanometer particles. Two-dimensional rectangular arrays of holes and wells have been also considered recently [26,27].

The grating we are investigating in this paper is just both 2D and dotted: it is an array of identical subwavelength particles located in a plane. Previously, in Refs. [28,29], we constructed the theory of SPR in the wave zone for a particular case of such a grating—a 2D rectangular grating (see Fig. 1). We demonstrated that in the case of a 2D rectangular grating SPR keeps its main features, but a certain complication of the diffraction pattern occurs, so the relation in Eq. (2) should be replaced by

$$d_y \sin\theta \sin\phi = s_y\lambda, \quad s_y = \cdots, -2, -1, 0, 1, 2, \ldots, \tag{6}$$

where d_y is the second period of the grating and the integer s_y is the associated diffraction order.

In contrast to the 1D case, the radiation intensity maxima are no longer concentrated near a certain single surface. This

FIG. 1. Scheme of a 2D rectangular grating with a passing electron.

spatial complex structure of radiation is believed to provide additional information for the beam diagnostics, better tuning, and control of radiation generation.

Below we present the theory of SPR generated from a 2D grating of subwavelength particles, valid in the prewave zone and the near zone. We also derive analytically the expression that describes how to arrange the elements of a 2D grating to focus SPR in the prewave zone.

III. THEORY OF SMITH-PURCELL RADIATION FROM SUBWAVELENGTH PARTICLES

The theory for the wave zone of the SPR generated by a 2D grating of subwavelength particles was constructed in [28,29]. For the theory to be extended to the prewave zone, and even for the near zone, it becomes possible to use the same approach. Now, however, we should take into account the terms that are no longer negligible at finite distances from the grating. Below we outline the concept of the theoretical model for the SPR from subwavelength particles.

We assume that only a single charge e is passing over the grating. Such one-particle consideration will make it possible in the future to describe the beam profile in detail. Using microscopic Maxwell's equations one can always express electric $\mathbf{E}$ and magnetic $\mathbf{H}$ fields via the total current density $\mathbf{j}^{tot}$. These relations are simpler for the Fourier transforms in variables $(\mathbf{q}, \omega)$:

$$\mathbf{E}(\mathbf{q}, \omega) = -\frac{4\pi i}{\omega}\frac{\mathbf{q}(\mathbf{q} \cdot \mathbf{j}^{\text{tot}}(\mathbf{q}, \omega)) - k^2\mathbf{j}^{\text{tot}}(\mathbf{q}, \omega)}{q^2 - k^2}, \quad (7)$$

$$\mathbf{H}(\mathbf{q}, \omega) = \frac{4\pi i}{c}\frac{[\mathbf{q} \times \mathbf{j}^{\text{tot}}(\mathbf{q}, \omega)]}{q^2 - k^2}, \quad (8)$$

where c is the speed of light in vacuum and k is the wave number, which is equal to ω/c. The problem is that the current density, in turn, is determined by the electromagnetic fields. To obtain the solution analytically, we can simplify this interconnection. The total current density consists of two parts: the current density of the passing charge $\mathbf{j}^0$ and the current density $\mathbf{j}$ excited in the grating. We can assume the passing charge e to be free, neglecting its energy loss during interaction with the grating,

$$\mathbf{j}^0(\mathbf{r}, t) = e\mathbf{v}\delta(\mathbf{r} - \mathbf{r}^0 - \mathbf{v}t), \quad (9)$$

where $\mathbf{v}$ is the constant velocity of the charge, $\mathbf{r}^0$ is its initial position, and δ is the Dirac delta function.

At the distances large in comparison with the size of subwavelength particles we still can use the dipole approximation to describe the other part of the current density,

$$\mathbf{j}(\mathbf{r}, t) = \frac{\partial}{\partial t}\sum_m \mathbf{d}_m(t)\delta(\mathbf{r} - \mathbf{r}_m), \quad (10)$$

where $\mathbf{d}_m$ is the dipole moment of the particle with index m located at the point $\mathbf{r}_m$; the sum is over all N particles the grating consists of. It is easy to establish the form of the dipole moments after introducing one more approximation: if the interaction between the particles is negligible then every dipole moment is determined by the free charge's Coulomb field $\mathbf{E}^0$ only:

$$\mathbf{d}_m(\omega) = \alpha(\omega)\mathbf{E}^0(\mathbf{r}_m, \omega), \quad (11)$$

where α is the polarizability of the particle.

For the charge e with initial position $\mathbf{r}^0 = (0, \ 0, \ h)$ moving along the OX axis, the spectral Fourier transform of the Coulomb field $\mathbf{E}^0$ is given by

$$\mathbf{E}^0(\mathbf{r}, \omega) = \exp\left(i\frac{kx}{\beta}\right)\frac{e\omega}{\pi v^2\gamma}$$
$$\times \left\{-iK_0\left(\frac{\rho\omega}{v\gamma}\right)\mathbf{e}_x + \gamma K_1\left(\frac{\rho\omega}{v\gamma}\right)\frac{\boldsymbol{\rho}}{\rho}\right\}, \quad (12)$$

where K_0 and K_1 stand for the modified Bessel functions of the first kind and of the zero and first orders, $\boldsymbol{\rho} = (0, y, z-h)$, and $\mathbf{e}_x$ is the unit vector along the OX axis.

Calculations of the inverse Fourier transform of Eqs. (7) and (8) read

$$\mathbf{E}(\mathbf{r}, \omega) = \sum_m \mathbf{d}_m\left(\frac{k^2}{R_m} + \frac{ik}{R_m^2} - \frac{1}{R_m^3}\right)e^{ikR_m}$$
$$+ \sum_m \mathbf{R}_m(\mathbf{R}_m \cdot \mathbf{d}_m)\left(-\frac{k^2}{R_m^3} - \frac{3ik}{R_m^4} + \frac{3}{R_m^5}\right)e^{ikR_m}, \quad (13)$$

and

$$\mathbf{H}(\mathbf{r}, \omega) = ik\sum_m(\mathbf{d}_m \times \mathbf{R}_m)\left(\frac{ik}{R_m^2} - \frac{1}{R_m^3}\right)e^{ikR_m}, \quad (14)$$

with $\mathbf{R}_m = \mathbf{r} - \mathbf{r}_m$ and $\mathbf{d}_m \equiv \mathbf{d}_m(\omega)$.

Since no assumptions have been made about the relation of the distance r to the dimensions of the radiating system or to the radiation wavelength, Eqs. (13) and (14) are applicable for all zones (wave, prewave, near).

It is easy to verify that the obtained general equation (13) agrees well with the theory for the wave zone [28,29]. Indeed, at far distances $(kr \gg 1)$ Eq. (13) reads

$$\mathbf{E}(\mathbf{r}, \omega)|_{kr \gg 1} = \sum_m \frac{k^2}{R_m^3}[\mathbf{R}_m \times (\mathbf{d}_m \times \mathbf{R}_m)]e^{ikR_m}. \quad (15)$$

For $r \gg L, M$ R_m should be expanded into a Taylor series:

$$R_m = r - (\mathbf{r}_m \cdot \mathbf{n}) + \frac{|\mathbf{r}_m \times \mathbf{n}|^2}{2r} + \ldots, \quad (16)$$

where $\mathbf{n}$ is a unit vector along $\mathbf{r}$. From Eq. (16) is easy to see how the wave zone criterion is obtained: if Eq. (3) is fulfilled, then, in the argument of the exponent in Eq. (15), one can neglect all the terms of the expansion of Eq. (16) but for the two first linear terms. Finally, for the wave zone we obtain

$$\mathbf{E}(\mathbf{r}, \omega)|_{r \gg \Re}$$
$$= \frac{k^2}{r}e^{ikr}\left[\left(\mathbf{n} \times \sum_m \mathbf{d}_m e^{-ik(\mathbf{n}\cdot\mathbf{r}_m)}\right) \times \mathbf{n}\right], \quad (17)$$

which coincides with the results of [28,29].

The theory constructed here does not consider interaction between the particles. It means that the influence from the neighboring particles is negligible, which needs the condition

$$(R_{\text{particle}}/R_{\text{between}})^3 \ll 1 \quad (18)$$

to be fulfilled; here R_{particle} is the size of the particle and R_{between} is the distance between two neighboring particles. For Eq. (18) is correct for the particles made of the material with

a not too high dielectric constant; in a more general situation, this criterion depends on the value of the dielectric constant. Interestingly, this estimation leads to the very close, qualitatively and numerically coinciding results both for the case of only two interacting particles (see Eqs. (10)–(12) in [30] and the conditions when the key coefficients V and W in Eq. (12) in [30] differ from unity), and for $N \gg 1$ interacting particles [31] (in this case it is called a local field effect; see the denominators in Eq. (21) in [31]). Yet, in the case of conditions of a resonance, the interaction between particles becomes crucial [30,31], especially when the distance between particles is subnanometers, when the quantum regime of tunneling changes the electromagnetic properties of coupled systems drastically [32]. In this study we do not consider the interaction between individual particles composing the 2D array, meaning that the distances between the particles considerably exceed nanometers, and that the particles are not in conditions of a resonance that require very fine, well-selected parameters. Besides theoretical estimations in [30,31], we demonstrated that the theory based on the assumption about noninteracting particles in a 2D array similar to the one considered here is able to describe the experimental data with very high precision [33].

Let us now calculate the radiation according to Eqs. (13) and (14) and discuss the properties of SPR from a 2D array in the prewave zone. In practice, of most interest is the region free of the moving electrons and their Coulomb field ($r \gg \gamma \lambda$). This region corresponds to the prewave zone. Therefore, in this paper we restrict our analysis to the prewave zone and leave the discussion of the near zone for the future.

To illustrate the characteristics of the radiation in the prewave zone we calculate the amount of energy passing through a sphere of finite radius r with a 2D grating in its center per unit solid angle and per unit frequency interval,

$$\frac{d^2 W(\mathbf{r}, \omega)}{d(\hbar \omega) d\Omega} = \frac{cr^2}{\hbar} \mathrm{Re}(\mathbf{n} \cdot [\mathbf{E}(\mathbf{r}, \omega) \times \mathbf{H}^*(\mathbf{r}, \omega)]), \qquad (19)$$

where $\mathbf{H}^*$ is the complex conjugate of $\mathbf{H}$.

Below we consider the radiation from a 2D rectangular grating having N_x rows along the OX axis and N_y rows along the OY axis. The polarizability of the particles α is assumed to be constant in the frequency range under consideration, which is reasonable until we are far from resonances caused by the denominators of α; for Fig. 2 we took the polarizability of a spherical particle of radius $a = 0.1$ mm made of material with the dielectric constant equal to 2.

Figure 2 demonstrates the angular dependences at four different distances: 23 m, 230 cm, 576 mm, and 72 mm. The first (black solid line) corresponds to the explicit wave zone; the second (blue dashed line) is equal to the parameter $\Re$ — a critical distance delimiting the wave and prewave zones [see Eq. (4)]; the third (green dotted line) is equal to $\gamma^2 \lambda$; and the last one (red dash-dotted line) is $3\gamma \lambda$ — the shortest distance from the grating at which space can still be considered free of the Coulomb field.

At the distance $r = \Re$ the radiation is close to that in the wave zone: the main peak decreases and broadens, but insignificantly. At the distance $r = \gamma^2 \lambda$ these changes become essential: the peak is twice as low, and the width is twice as
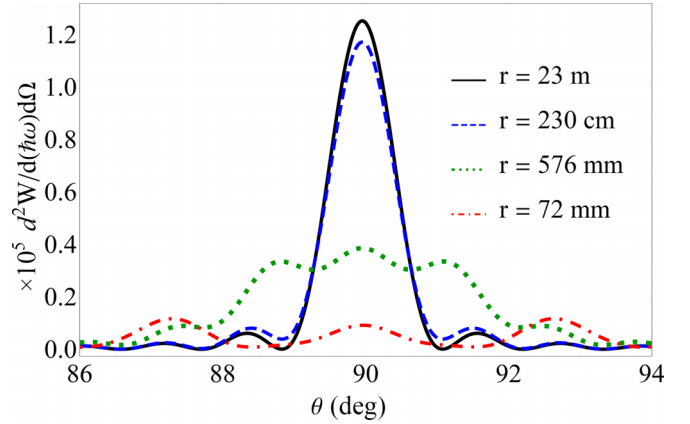

FIG. 2. The polar distribution of SPR at four different distances r. Parameters: $\lambda = 1$ mm, $\phi = 3°$, $d_x = 3$ mm, $d_y = 2$ mm, $N_x = 17$, $N_y = 13$, $h = 1$ mm, $\alpha = 25 \times 10^{-5}$ mm^3, $\gamma = 24$.

large. Finally, at the distance $r = 3\gamma \lambda$, the radiation loses the form of pronounced peaks characteristic of the wave zone.

Similarly, the radiation intensity given by Eq. (19) behaves in the spectral region; see Fig. 3. In the prewave zone radiation is significantly less monochromatic than in the wave zone. In contrast to the angular dependence, the spectral intensity peak not only broadens with decreasing r, but also becomes asymmetric. In fact, this asymmetry is present in the wave zone as well, both due to the factor k^6 and the Coulomb field dependence on k through the Bessel functions. The broadening of the peak in the prewave zone only reveals this asymmetry.

These prewave zone effects for a 2D grating are very similar to the conventional grating effects described in [22]. The spectral and spatial broadening of radiation peaks in the prewave zone is a common feature of both transition and diffraction radiation. This is called the "defocusing effect," which is characteristic of the prewave zone.
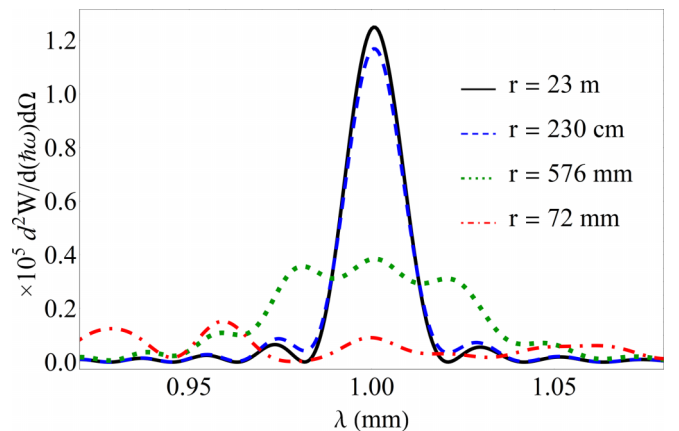

FIG. 3. The spectral distribution of SPR at four different distances r. Parameters: $\theta = 90°$, and the others (except for the λ) are like in Fig. 2.

IV. GENERALIZED DISPERSION RELATION

For the radiation to be maximum at the point of observation, the phase difference between the signals from a fixed particle of the grating and all the others must be a multiple of 2π. For convenience, we fix the particle with index "1" and place it in the origin of the coordinate system ($R_1 = r$). The condition for the maximum of radiation then might be written as a system of $N-1$ equations for the radius vector $\mathbf{r}$,

$$\beta^{-1}x_m + R_m = r + s_m\lambda, \quad m = 2, 3, \ldots, N, \quad (20)$$

where s_m is an arbitrary integer, individual for every particle (but not necessarily unique).

Unlike the conventional dispersion relations valid for the wave zone, the solutions of Eq. (20), if they exist, define not only directions of the most intense radiation, but the points of its concentration in the prewave zone and the near zone. This generalized dispersion relation contains the location of every single particle.

To verify that for a 2D rectangular grating system, (20) transforms into the conventional dispersion relations in the wave zone, we can use the Taylor series expansion of R_m again. Then Eq. (20) might be written as follows:

$$\beta^{-1}x_m - (\mathbf{n} \cdot \mathbf{r}_m) = s_m\lambda, \quad m = 2, 3, \ldots, N. \quad (21)$$

In a rectangular grating with periods d_x and d_y the radius vector of a particle $\mathbf{r}_m$ is expressed as

$$\mathbf{r}_m = m_x d_x \mathbf{e}_x + m_y d_y \mathbf{e}_y, \quad (22)$$

with integers m_x and m_y being the numbers of rows along the grating axes. Then Eq. (21) reads

$$m_x d_x(\beta^{-1} - \cos\theta) - m_y d_y \sin\theta \sin\phi = s_m\lambda,$$
$$m = 2, 3, \ldots, N. \quad (23)$$

This system of $N-1$ equations is absolutely equivalent to a system of two dispersion relations; see Eqs. (1) and (6):

$$d_x(\beta^{-1} - \cos\theta) = s_x\lambda$$
$$d_y \sin\theta \sin\phi = s_y\lambda. \quad (24)$$

Indeed, any equation of the system in Eq. (23) is just a linear combination of the two equations from Eq. (24).

V. RADIATION FOCUSING

From the dispersion relations it is easy to perceive the reason of the defocusing effect: if a 2D rectangular grating fulfills Eq. (21) for an infinitely distant point, then it principally cannot fulfill Eq. (20) for a finite distant point in the same direction due to the appearance of additional terms of expansion in Eq. (16). The conditions for the pure interference are broken, both for the constructive and destructive one. As a result, SPR intensity peaks decrease and broaden.

From this consideration, we can propose how to suppress the defocusing effect in the prewave zone. Usually, additional and special optics is used for that (using lenses [34] or concave mirrors [35]), but it is possible to achieve the same or even better effect (better, because there will be no distortion from additional optical elements) based on rearranging the positions of the individual particles that make up a 2D array.

For solid nonperiodic gratings (which exclude consideration of SPR), there is a way close to what we suggest in this study: to change the form of the target so that the radiation from it could be concentrated. The focusing of transition radiation of relativistic electrons with parabolic surfaces was first proposed by Ryazanov and Tilinin [36], who used an analogy with optic devices. Although their pioneering paper [36] was about focusing of the radiation at large distances, much later this effect of focusing was explored to suppress the prewave zone effect. This effect was verified experimentally for the electrons of moderate energy [37], and after that the focusing with concave [38] and spherical [39] targets was investigated as well. The only study for a periodic structure (1D, a conventional diffraction grating), applicable for focusing of SPR, was conducted experimentally by Naumenko with coauthors for a parabolic geometry [40]. In [41] we also attempted to consider the spherical geometry for the SPR focusing, but the effect was almost invisible, and below we show why: the law of arranging the particles' locations proves to be nonspherical.

The idea to change the target form to suppress the prewave zone effect seems to be the most prospective and interesting, as this method does not bring frequency limitation and does not require an additional focusing system, bringing additional distortions. Although in [37–40] successful radiation focusing was reported, the question about the choice of topology of the target remains open (parabolic, hyperbolic, spherical?, or another form?). Thus, the topology of the focusing grating for SPR is an open problem; for the 2D gratings (like photonic crystals, including photonic crystal slabs, metagratings, metasurfaces) this problem has not been considered yet. Below, on the basis of the theory constructed above, we investigate this issue. We will proceed from the fact that Eq. (20) makes it possible not only to determine the points in space at which the radiation is maximal, but, vice versa, to find the grating topology, in which the radiation is maximum at the selected point.

If we square Eq. (20) with a fixed s_m and consider it as an equation for $\mathbf{r}_m$, it turns out to determine one of the two sheets of a circular hyperboloid:

$$\frac{(y_m - y)^2}{b_m^2} + \frac{(z_m - z)^2}{b_m^2} - \frac{(x_m - a_m)^2}{\gamma^2\beta^2 b_m^2}$$
$$= -1 x_m < \beta(r + \lambda s_m), \quad (25)$$

where

$$a_m = \beta\gamma^2(r + s_m\lambda - \beta x),$$
$$b_m = \gamma(\beta r + \beta s_m\lambda - x). \quad (26)$$

One can see that the major axis of the hyperboloid sheet is parallel to the particle's trajectory. The surface is concave towards the approaching charge. The focus of the sheet is the point with radius vector $\mathbf{r}$. The hyperboloid sheets of Eq. (25) corresponding to different integers s_m have different curvatures and are embedded one into another; the vertices of the sheets are not located periodically. In [19], for a 1D grating, a qualitative indication of the hyperbolic law was also obtained, but without calculating of SPR radiation field or intensity characteristics.

For the limiting case of infinite Lorentz factor $\gamma \to \infty$ Eq. (20) corresponds to a paraboloid,

$$(y_m - y)^2 + (z_m - z)^2 = -c_m(x_m - d_m)$$
$$x_m < r + \lambda s_m, \qquad (27)$$

with

$$c_m = 2(r + \lambda s_m - x),$$
$$d_m = (r + \lambda s_m + x)/2. \qquad (28)$$

The electron moves parallel to the major axis of the paraboloid. We recall that the same scheme was proposed in [36] for transition radiation from relativistic electrons. In optics, the parabolic mirrors are well known to focus plane waves that move along its axis. This fact agrees well with our result and Ryazanov's prediction, since the field of a relativistic particle is similar to a plane wave and the virtual photon approximation is often used to describe the radiation processes. The paraboloids determined by Eq. (27) with different s_m are embedded one into another with their vertices located periodically.

To construct a plane grating, we should take a corresponding section of the set of the surfaces defined by Eq. (25) or (27). Let the plane be $z_m = 0$. The result is obviously the set of hyperbolas (and parabolas for ultrarelativistic electrons). In contrast to the parabolic gratings considered by Naumenko [40], the axes of our parabolas are parallel rather than perpendicular to the particle's trajectory.

Of considerable interest is also the condition for the essential curvature of the hyperbolic rows. This can be formulated as the comparability of the transverse size of the grating M with the value of the minor semiaxis of the hyperboloid b_m. Assuming that the transverse size of the array is comparable with the size of the effective field, we roughly obtain

$$r = \lambda. \qquad (29)$$

Hence, a hyperbolic array, ideally, should be used at distances of the order of the radiation wavelength, which corresponds to the near zone; yet, as we will demonstrate below, it works well for farther distances in the prewave zone as well.

We consider 2D particle arrays, while the obtained hyperbolas are continual lines. To construct a focusing 2D array, we place the particles along the hyperbolas at a fixed distance d_y between them along the OY axis. Taking the parameters d_y, λ, γ, N_x, and N_y used for Fig. 2, below we demonstrate the view of the hyperbolic 2D arrays focusing directly above their centers $\mathbf{r} = (0, \ 0, \ r)$ at distances $r = \gamma^2 \lambda$ and $r = 3\gamma\lambda$; see Figs. 4 and 5, correspondingly.

In Fig. 4, the black rings correspond to the particles of the initial rectangular array, while green circles correspond to the focusing array with the changed particles' positions. In the central region the circles and rings overlap well. A significant shift of circles is seen on the left and right edges of the grating. Although for the parameters taken this is more like a parallel shift of outer rows to the left, the true position of the green circles is described by the hyperbolic law. Such a topology recalls the varied line-space gratings widely used in spectrometry both to disperse and to focus radiation [42]. For the distance $r = 3\gamma\lambda$, the bent array (red circles) becomes distinct from a rectangular one (black rings) (see Fig. 5); i.e.,
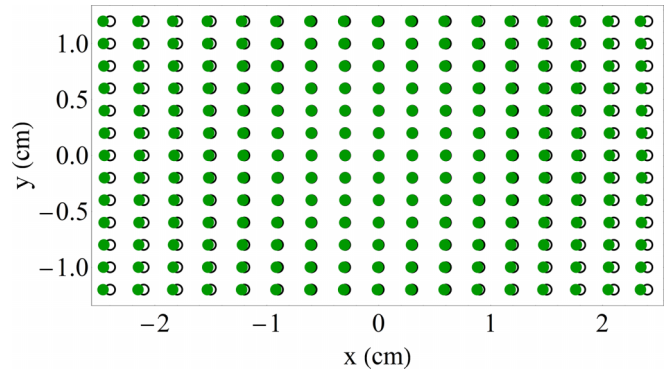

FIG. 4. A scheme of 2D arrays. Black rings: a rectangular array; green circles: a hyperbolic array with the focus at $r = \gamma^2\lambda = 576$ mm; other parameters are like in Fig. 2. For clarity, the array is shown not at scale: the particles' radius is shown in a 2.25 times larger scale.

to focus the radiation nearer to the surface, one should take more curved rows.

Figure 6 presents the angular dependence of intensity from the arrays focusing SPR at different distances.

In contrast to the rectangular grating (Fig. 2), radiation curves of focusing gratings for different distances practically coincide starting from $r = \gamma^2\lambda = 576$ mm and farther. For the distinction to be observed, one must examine the peak carefully. Nevertheless, for $r = 3\gamma\lambda$ the defocusing effect still takes place as the red dash-dotted curve broadens and decreases, albeit insignificantly (compare with Fig. 2). It means that the hyperbolic design of the grating allows getting typical wave zone spatial properties of the SPR near one of its chosen peaks in essentially the prewave zone. It seems interesting that such small changes in the array topology lead to such significant changes in the radiation intensity distribution depending on the distance at which the radiation is observed.

VI. EFFECT OF PARTICLE POSITION IRREGULARITY

Now let us discuss the influence of the particle position irregularity on radiation distributions, which can appear during manufacturing of the arrays. For this purpose we calculate the radiation intensity from a hyperbolic array, each particle of which is randomly shifted from its exact location according to
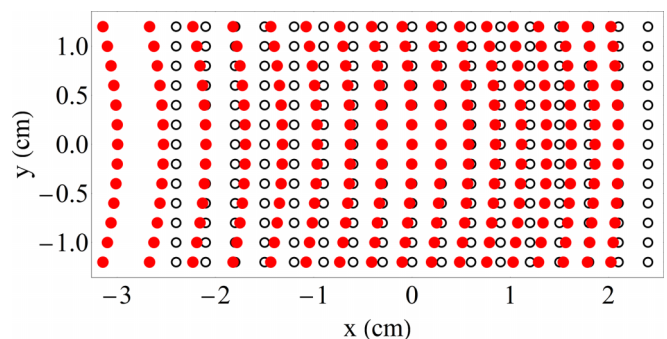

FIG. 5. The same as in Fig. 4, but the red circles correspond to the hyperbolic grating with the focus at $r = 3\gamma\lambda = 72$ mm.
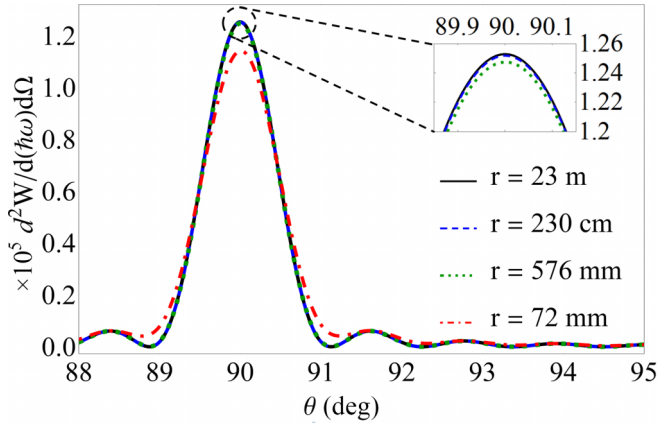
FIG. 6. The polar distribution of SPR at four different distances r from a hyperbolic array. The other parameters (except for d_x) are like in Fig. 2.
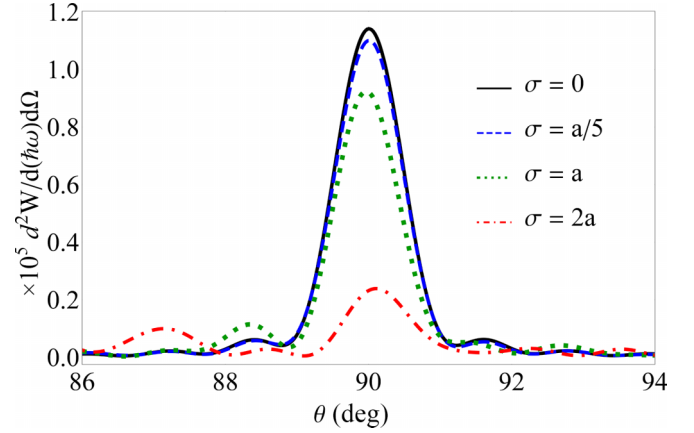

FIG. 8. The polar distribution of SPR from a hyperbolic array with focus at $r = 72$ mm and four different values of the deviation σ; other parameters are like in Fig. 2.

Gaussian distribution with standard deviation σ (see Fig. 7), and see how it will affect the focusing.

In Fig. 8 we demonstrate the polar distribution of SPR from hyperbolic irregular gratings with four different deviations defining random Gaussian noise. For clarity, we value the standard deviation σ according to the particles' radius a. One can see that the defocusing effect caused by irregularity is significant for deviations comparable to the particles' radius and larger (see the green dotted and red dash-dotted curves in Fig. 8). The existing technologies allow manufacturing of the arrays with much higher accuracy: e.g., for the parameters close to those used in Fig. 2 a similar array was manufactured, see [33], with accuracy in the particles' positions about 2 microns and for the particle radius about 150 microns. Therefore, it is correct to expect that in practice the accuracy of manufacturing will not be a problem: Fig. 8 clearly demonstrates that for such small mean deviations the defocusing effect is

negligible. Figure 7 illustrates a particular concrete case of a focusing array, for which Fig. 8 shows a strong defocusing effect due to irregularities in the particles' position: it happens if the standard deviation σ is twice as large as the particles' radius; i.e., the array in Fig. 7 corresponds to the red dash-dotted curve in Fig. 8.

VII. CONCLUSION

In this study we considered Smith-Purcell radiation from flat arrays constructed of single particles. The analytic theory of SPR from 2D gratings was constructed for the prewave zone. Similarly to SPR from conventional gratings our results show that at distances comparable to the wave zone criterion, the radiation properties from a 2D grating are very close to those of the wave zone. In the prewave zone, however, significant distinctions occur.
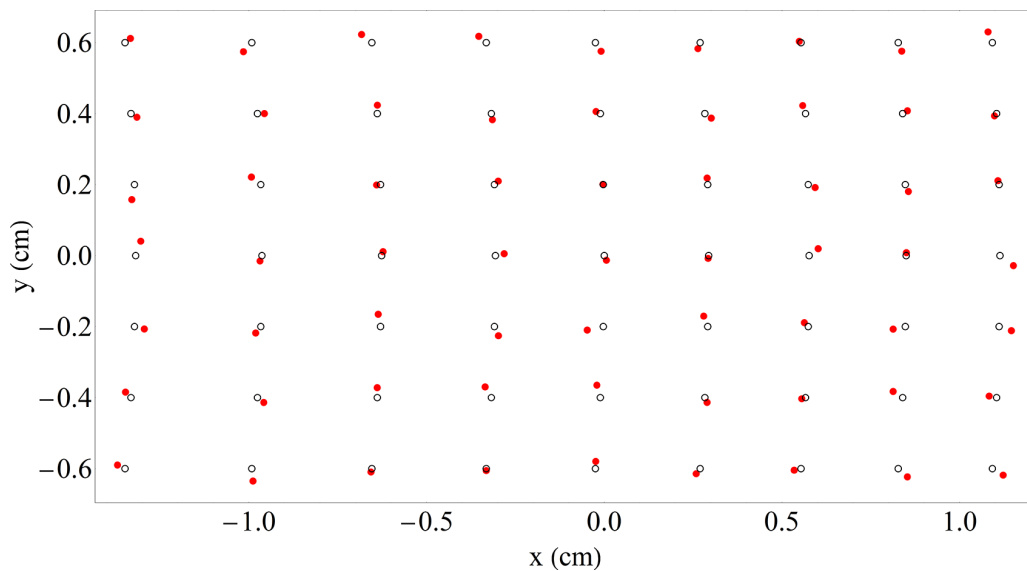

FIG. 7. Scheme of a part of the 2D arrays with focus at $r = 72$ mm; contrary to Figs. 4 and 5, this scheme is in scale. Black rings: a hyperbolic regular array; red circles: hyperbolic irregular array with $\sigma = 2a$; other parameters are like in Fig. 2.

A generalized dispersion relation for SPR has been obtained. It allows tailoring the topology of the grating determining the positions of its individual elements, so that the grating can focus the radiation at chosen points in space. The analysis shows that hyperbolic and parabolic arrangement plays a key role in designing the topology of such 2D gratings in view of their focusing properties. Although the focusing design was obtained for dotted gratings of subwavelength particles it is applicable for continual 1D gratings of narrow strips.

Although, as we have shown, the irregularities of the manufactured structure can lead to defocusing, our numerical simulations demonstrate that the effect of defocusing caused by the Gaussian noise in the positions of single particles is negligible for the accuracy provided by existing level of technologies.

There is one more interesting issue about the prewave zone effect. Although this effect is classical, it can play an important role in revealing the quantum wave nature through spontaneous emission of free electrons due to the close analogy between the zone of formation of radiation determined by the classical coherence effects, and the delocalized size of the wave packets describing quantum electrons and radiation beams; details of this interesting recent discussion can be found in [43–47]. Then the effect of focusing in the prewave zone can be important in view of possible experiments on this problem.

[1] S. J. Smith and E. M. Purcell, Visible light from localized surface charges moving across a grating, Phys. Rev. **92**, 1069 (1953).

[2] V. P. Shestopalov, *The Smith-Purcell Effect* (Nova Science Publishers, Commack, NY, 1998).

[3] A. P. Potylitsyn, M. I. Ryazanov, M. N. Strikhanov, and A. A. Tishchenko, *Diffraction Radiation from Relativistic Particles, Springer Tracts in Modern Physics* (Springer, Berlin, 2010), Vol. 239.

[4] M. C. Lampel, Coherent Smith-Purcell radiation as a pulse length diagnostic, Nucl. Instrum. Methods Phys. Res. Sect. A **385**, 19 (1997).

[5] H. Andrews, F. B. Taheri, J. Barros, R. Bartolini, V. Bharadwaj, C. Clarke, N. Delerue, G. Doucas, N. Fuster-Martinez, M. Vieille-Grosjean, I. Konoplev, M. Labat, S. L. Corre, C. Perry, A. Reichold, and S. Stevenson, Reconstruction of the time profile of 20.35 GeV, subpicosecond long electron bunches by means of coherent Smith-Purcell radiation, Phys. Rev. Spec. Top.–Accel. Beams **17**, 052802 (2014).

[6] I. V. Konoplev, G. Doucas, H. Harrison, A. J. Lancaster, and H. Zhang, Single shot, nondestructive monitor for longitudinal subpicosecond bunch profile measurements with femtosecond resolution, Phys. Rev. Accel. Beams **24**, 022801 (2021).

[7] P. Heil, K. Aulenbacher, C. Matejcek, S. Friederich, M. Bruker, and F. Fichtner, Coherent Smith-Purcell radiation for minimally invasive bunch length measurement at the subpicosecond time scale, Phys. Rev. Accel. Beams **24**, 042803 (2021).

[8] Z. Su, F. Cheng, L. Li, and Y. Liu, Complete control of Smith-Purcell radiation by grapheme metasurfaces, ACS Photon. **6**, 1947 (2019).

[9] L. Jing, D. Liao, J. Tao, H. Chen, and Z. Wang, Generation of Airy beams in Smith–Purcell radiation, Opt. Lett. **47**, 2790 (2022).

[10] R. Remez, N. Shapira, C. Roques-Carmes, R. Tirole, Y. Yang, Y. Lereah, M. Soljačić, I. Kaminer, and A. Arie, Spectral and spatial shaping of Smith-Purcell radiation, Phys. Rev. A **96**, 061801(R) (2017).

[11] A. Karnieli, D. Roitman, M. Liebtrau, S. Tsesses, N. Van Nielen, I. Kaminer, A. Arie, and A. Polman, Cylindrical metalens for generation and focusing of free-electron radiation, Nano Lett. **22**, 5641 (2022).

[12] I. Kaminer, S. E. Kooi, R. Shiloh, B. Zhen, Y. Shen, J. J. López, R. Remez, S. A. Skirlo, Y. Yang, J. D. Joannopoulos, A. Arie, and M. Soljacic, Spectrally and spatially resolved Smith-Purcell radiation in plasmonic crystals with short-range disorder, Phys. Rev. X **7**, 011003 (2017).

[13] N. Talebi, S. Meuret, S. Guo, M. Hentschel, A. Polman, H. Giessen, and P. A. van Aken, Merging transformation optics with electron-driven photon sources, Nat. Commun. **10**, 599 (2019).

[14] C. Roques-Carmes, S. E. Kooi, Y. Yang, N. Rivera, P. D. Keathley, J. D. Joannopoulos, S. G. Johnson, I. Kaminer, K. K. Berggren, and M. Soljačić, Free-electron-light interaction in nanophotonics, Appl. Phys. Rev. **10**, 011303 (2023).

[15] Z. Wang, K. Yao, M. Chen, H. Chen, and Y. Liu, Manipulating Smith-Purcell emission with Babinet metasurfaces, Phys. Rev. Lett. **117**, 157401 (2016).

[16] X. Shi, M. Shentcis, Y. Kurman, L. J. Wong, F. J. García de Abajo, and I. Kaminer, Free-electron-driven x-ray caustics from strained van der Waals materials, Optica **10**, 292 (2023).

[17] S. N. Galyamin and A. V. Tyukhtin, Dielectric concentrator for Cherenkov radiation, Phys. Rev. Lett. **113**, 064802 (2014).

[18] A. V. Tyukhtin, S. N. Galyamin, V. V. Vorobev, and A. A. Grigoreva, Cherenkov radiation of a charge flying through the inverted conical target, Phys. Rev. A **102**, 053514 (2020).

[19] Y. Liu, W. Liu, L. Liang, Q. Jia, L. Wang, and Y. Lu, Threshold-less and focused Cherenkov radiations using sheet electron-beams to drive sub-wavelength hole arrays, Opt. Express **26**, 34994 (2018).

[20] F. S. Rusin and G. D. Bogomolov, The orotron, an electronic device with an open resonator and a reflecting grating, Radiophys. Quantum Electron. **11**, 430 (1968).

[21] V. A. Verzilov, Transition radiation in the pre-wave zone, Phys. Lett. A **273**, 135 (2000).

[22] D. V. Karlovets and A. P. Potylitsyn, Smith-Purcell radiation in the "pre-wave" zone, JETP Lett. **84**, 489 (2007).

[23] J. D. Jackson, *Classical Electrodynamics* (John Wiley & Sons, New York, 1962).

[24] N. E. Glass, Enhanced Smith-Purcell radiation from a bigrating, Phys. Rev. A **36**, 5235 (1987).

[25] F. J. García de Abajo, Smith-Purcell radiation emission in aligned nanoparticles, Phys. Rev. E **61**, 5743 (2000).

[26] L. Liang, W. Liu, Y. Liu, Q. Jia, L. Wang, and Y. Lu, Multi-color and multidirectional-steerable Smith-Purcell radiation from 2D sub-wavelength hole arrays, Appl. Phys. Lett. **113**, 013501 (2018).

[27] P. Zhang, L. Wang, Y. Zhang, A. Aimidula, and M. Tang, Intensive vertical orientation Smith-Purcell radiation from the 2D well-array metasurface, Opt. Express **27**, 3952 (2019).

[28] D. Yu. Sergeeva, A. A. Tishchenko, and M. N. Strikhanov, Microscopic theory of Smith-Purcell radiation from 2D photonic crystal, Nucl. Instrum. Methods Phys. Res. Sect. B **402**, 206 (2017).

[29] D. I. Garaev, D. Yu. Sergeeva, and A. A. Tishchenko, Theory of Smith-Purcell radiation from a 2D array of small noninteracting particles, Phys. Rev. B **103**, 075403 (2021).

[30] A. A. Tishchenko and D. Yu. Sergeeva, Near-field resonances in photon emission via interaction of electrons with coupled nanoparticles, Phys. Rev. B **100**, 235421 (2019).

[31] M. I. Ryazanov, M. N. Strikhanov, and A. A. Tishchenko, Local field effect in diffraction radiation from a periodical system of dielectric spheres, Nucl. Instrum. Methods Phys. Res. Sect. B **266**, 3811 (2008).

[32] K. J. Savage, M. M. Hawkeye, R. Esteban, A. G. Borisov, J. Aizpurua, and J. J. Baumberg, Revealing the quantum regime in tunnelling plasmonics, Nature (London) **491**, 574 (2012).

[33] D. Yu. Sergeeva, A. S. Aryshev, A. A. Tishchenko, K. E. Popov, N. Terunuma, and J. Urakawa, THz Smith–Purcell and grating transition radiation from metasurface: Experiment and theory, Opt. Lett. **46**, 544 (2021).

[34] P. Karataev, Pre-wave zone effect in transition and diffraction radiation: Problems and solutions, Phys. Lett. A **345**, 428 (2005).

[35] B. N. Kalinin, G. A. Naumenko, A. P. Potylitsyn, G. A. Saruev, L. G. Sukhikh, and V. A. Cha, Measurement of the angular characteristics of transition radiation in near and far zones, JETP Lett. **84**, 110 (2006).

[36] M. I. Ryazanov and I. S. Tilinin, Transition radiation emitted by an ultrarelativistic particle crossing a curved interface between media, Sov. Phys. JETP **44**, 1092 (1976).

[37] G. A. Naumenko, V. A. Cha, B. N. Kalinin, Yu. A. Popov, A. P. Potylitsyn, G. A. Saruev, and L. G. Sukhikh, Focusing of transition radiation from a paraboloidal target, Nucl. Instrum. Methods Phys. Res. Sect. B **266**, 3733 (2008).

[38] A. P. Potylitsyn and R. O. Rezaev, Focusing of transition radiation and diffraction radiation from concave targets, Nucl. Instrum. Methods Phys. Res. Sect. B **252**, 44 (2006).

[39] L. G. Sukhikh, A. S. Aryshev, P. V. Karataev, G. A. Naumenko, A. P. Potylitsyn, N. Terunuma, and J. Urakawa, Observation of focusing effect in optical transition and diffraction radiation generated from a spherical target, Phys. Rev. Spec. Top. Accel. Beams **12**, 071001 (2009).

[40] G. A. Naumenko, A. P. Potylitsyn, L. G. Sukhikh, and Y. U. A. Popov, Experimental investigation of Smith–Purcell radiation focusing by using the parabolic gratings, Int. J. Mod. Phys. A **25**, 217 (2010).

[41] D. Yu. Sergeeva, A. A. Tishchenko, A. S. Aryshev, and M. N. Strikhanov, Smith-Purcell radiation from concave dotted gratings, J. of Instrum. **13**, C02045 (2018).

[42] E. A. Vishnyakov, A. S. Kolesnikov, A. O. Pirozhkov, E. N. Ragozin, and A. N. Shatokhin, Aperiodic reflection diffraction gratings for soft x-ray radiation and their application, Quantum Electron. **48**, 916 (2018).

[43] R. Remez, A. Karnieli, S. Trajtenberg-Mills, N. Shapira, I. Kaminer, Y. Lereah, and A. Arie, Observing the quantum wave nature of free electrons through spontaneous emission, Phys. Rev. Lett. **123**, 060401 (2019).

[44] D. V. Karlovets and A. M. Pupasov-Maksimov, Nonlinear quantum effects in electromagnetic radiation of a vortex electron, Phys. Rev. A **103**, 012214 (2021).

[45] A. Karnieli, R. Remez, I. Kaminer, and A. Arie, Comment on "Nonlinear quantum effects in electromagnetic radiation of a vortex electron", Phys. Rev. A **105**, 036202 (2022).

[46] D. V. Karlovets and A. M. Pupasov-Maksimov, Reply to "Comment on 'Nonlinear quantum effects in electromagnetic radiation of a vortex electron'", Phys. Rev. A **105**, 036203 (2022).

[47] A. Pupasov-Maksimov and D. Karlovets, Passage of a vortex electron over an inclined grating, Phys. Rev. A **105**, 042206 (2022).